J Mol Model (2007) 13:699–713
DOI 10.1007/s00894-007-0202-y

ORIGINAL PAPER

Ion conductance vs. pore gating and selectivity in KcsA channel: Modeling achievements and perspectives

Céline Boiteux · Sebastian Kraszewski · Christophe Ramseyer · Claude Girardet

Received: 16 November 2006 / Accepted: 19 March 2007 / Published online: 6 April 2007

Abstract KcsA potassium channel belongs to a wide family of allosteric proteins that switch between closed and open states conformations in response to a stimulus, and act as a regulator of cation activity in living cells. The gating mechanism and cation selectivity of such channels have been extensively studied in the literature, with a revival emphasis these latter years, due to the publication of the crystallized structure of KcsA. Despite the increasing number of research and review papers on these topics, quantitative interpretation of these processes at the atomic scale is far from achieved. On the basis of available experimental and theoretical data, and by including our recent results, we review the progresses in this field of activity and discuss the weaknesses that should be corrected. In this spirit, we partition the channel into the filter, cavity, extra and intracellular media, in order to analyze separately the specificity of each region. Special emphasis is brought to the study of an open state for the channel and to the different properties generated by the opening. The influence of water as a structural and dynamical component of the channel properties in closed and open states, as well as in the sequential motions of the cations, is analyzed using molecular dynamics simulations and *ab initio* calculations. The polarization and charge transfer effects on the ions' dynamics and kinetics are discussed in terms of partial charge models.

Keywords Ionic channels · Selectivity · Gating
Molecular dynamics · Ab initio calculations

C. Boiteux · S. Kraszewski · C. Ramseyer · C. Girardet (✉)
Laboratoire de Physique Moléculaire UMR CNRS 6624,
Université de Franche-Comté,
La Bouloie,
25030 Besançon Cedex, France
e-mail: claude.girardet@univ-fcomte.fr

Introduction

Ion channels are proteins inserted in the membrane lipidic bilayer of a cell which form aqueous pores. They allow ions to cross the hydrophobic barrier of the core membrane, guaranteeing to the cell exchange of ionized particles. There are many different families of ion channels which all possess the same basic properties. They can open or close the ion conduction in a controlled way and they are furthermore selective to an ion or to a range of ions. The first property corresponds to the gating, the second to the selectivity.

The gating mechanism was set in the late 1960s, with Armstrong's studies on voltage dependent channels, showing that ammonium compounds blocked potassium currents [1]. Important improvements in the knowledge of the gating were done in the late 1990s, when the x-ray structure of the transmembrane part of the bacterial potassium channel KcsA was established [2] and, a few years later, when the open form of the MthK channel was compared to the KcsA structure [3, 4]. At the same time, Electron Paramagnetism Resonance (EPR) and Site Directed Spin Labelling (SDSL) methods provided, together with restrained energy minimization of the structure, a model for the 3D fold of full-length KcsA including N and C termini in the cytoplasmic region [5]. It was suggested that, while these termini do not play a fundamental role in ion permeation, they could act as sensors to modulate the pH-dependent gating of the channel [5]. Then, the gating of a voltage dependent Kv channel was explored in the context of the MthK structure to determine the nature and magnitude of the structural changes induced by the gate opening [3–7]. Very recently, it has been shown that to open the conduction pathway of KcsA, two gates at least should act simultaneously [8–11]. This illustrates the difficulty in presently understanding the

gating mechanism, which seems not to be unique for all the potassium channels [12, 13].

The selectivity of sodium ion channels was experimentally revealed at nearly the same time as the investigations on the gating mechanism [14, 15], and it was then evidenced for the potassium channels a few years later [16, 17]. An attempt has been made to interpret the origin of this process in terms of differences in the coordination cage for K^+ and Na^+ ions in the channel. Such a model was then exploited on the basis of more precise information on the KcsA structure [2] and widely used in several studies based on molecular dynamics (MD) or brownian dynamics (BD) simulations [18–22]. Other hypotheses implying the ion hydration/dehydration mechanism at the mouths of the channel were also proposed [23]. Transition state theory has also been exploited to describe the ion transport and selectivity by determining the free energy variation for an ion entering the filter [24–27]. Unfortunately, no well-established microscopic mechanism can actually explain the selectivity of potassium channels.

Several interesting reviews on the potassium channels occurred since 2000, which all describe in detail the progresses carried out on our understanding of gating and selectivity mechanisms, either based on experimental arguments, especially by comparing pH and voltage-gated channels [28–30], or based on calculations [31–35]. The goal of this paper is to introduce, in the discussion of these reviews, additional information obtained from molecular dynamics and quantum calculations on the KcsA. These additional data concern the ions correlation in the permeation mechanism and the influence of water on the ionic conduction. These topics were widely discussed for the closed state of the K channel, and they are extended here to an atomic description of an open state. They also describe polarization effects on ions and protein walls, especially the occurrence of different partial charges on K^+ and Na^+ ions, which could be at the origin of channel selectivity.

Basis of the channel structure

General information from experiments

The primary function of an ion channel is thus to permit the controlled and selective diffusion of ions across the membrane from the cell interior to the extracellular medium. Understanding this feature requires atomistic information on the protein structure embedded in the lipidic membrane. Such information, although still partial, is available for a small set of voltage and ligand-gated ion channels [6, 36, 37] and has reached a high standard for the KcsA channel, with the x-rays crystallized structure at 2.0 Å resolution (pdb 1K4C) [38], 3 years after a previously published structure at a lower resolution by the same group (pdb 1BL8) [2].

The basic structure of KcsA consists of four subunits that form a symmetric tetramer (Fig. 1a). Each subunit is made up of one outer (M_1) and one inner (M_2) transmembrane helices connected by a re-entrant P loop (Fig. 1b), made by a descending P helix and an ascending F region containing the TVGYG (Threonine, Valine, Glycine, Tyrosine, Glycine) sequence common to all K^+ channels [39–41] and responsible for selectivity [42] (Fig. 2). This latter region forms the filter at the outermost part of the membrane. This narrow part, of radius 1.4 Å and around 12 Å long, opens on a rather large outer mouth limited by the M_2 helices, which form an inverted tepee-like structure at the intracellular part of the pore. The widest part of this structure consists of a hydrated cavity C, which can be approximated by a sphere of 5–6 Å radius forming the inner vestibule, while the narrowest part corresponds to the gate G with a radius of about 2 Å (Fig. 2a). The cytoplasmic part is constituted by NH_2 termini which form α-helices anchored at the membrane-water interface, while the COOH termini form a right-handed four helices bundle that extend towards the cell cytoplasm (Fig. 3).

Fifty years before the experimental determination of the channel structure by MacKinnon and collaborators [2], Hodgkin and Keynes [43] had shown that the filter contains two to three K^+ ions and that permeation involves single-file ion motions across the membrane (Fig. 2b). Such a feature has been corroborated by the x-ray data, and information on the ion sites in the entire pore is now relatively well-established [44, 45]. Seven sites have been determined at relatively high K^+ concentration, S_{ext} and S_0 located at the outer mouth of the filter, S_1 to S_4 inside the filter and S_{cav} in the cavity [40, 46]. S_1 to S_4 are between planes defined by carbonyl and hydroxyl oxygen atoms of Y78, C77, V76 and T75 residues in such a way each K^+ ion is solvated by 8 oxygen atoms.

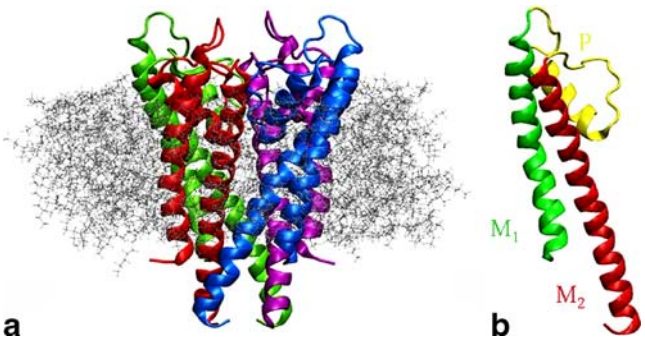

Fig. 1 **a** Structure of the KcsA protein embedded in the octane slab mimicking the lipid membrane. The four subunits forming the channel are drawn in different colors. **b** Structure of one monomer formed by the two transmembrane helices M_1 and M_2, and the P loop

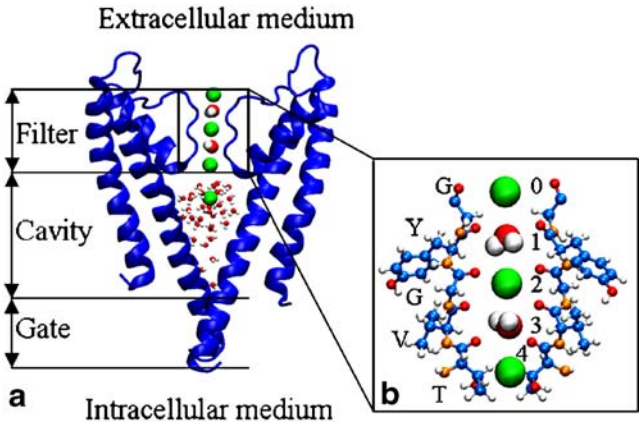

Fig. 2 **a** Partition of the closed state of the channel, using only two monomers for clarity. *Green circles* represent cations, in alternation with water molecules (oxygen in *red* and hydrogen in *white*). **b** Zoom of the filter part describing the TVGYG sequence. Sites created by carbonyl groups are labelled by number 0 to 4 (carbon in *blue*)

Numerical methods

Using structural data, theoretical approaches can help the confirmation of experimental models on the permeation dynamics, channel conductance and selectivity [46]. Two limiting factors prevent an accurate development of theoretical methodologies. Firstly, the number of atoms that can be considered in these approaches to interpret permeation and gating mechanisms is in general too small regarding the size of the protein and the closer parts of the membrane. Secondly, times which are relevant to describe the gating and the ion diffusion through the pore are very long when compared to the ion dynamics.

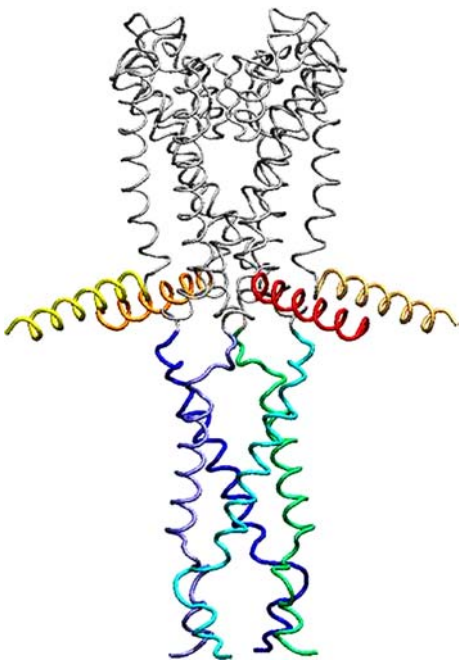

Fig. 3 Full-length KcsA structure including the cytoplasmic region (pdb 1F6G). N (from *yellow* to *red*) and C (from *green* to *blue*) termini are shown on this figure, in addition to the membrane part (in *grey*) of the KcsA

Ab initio calculations based on first principles are therefore unable to describe these phenomena since the maximum number of involved atoms ($<10^3$) is dramatically small when compared to the system size ($\geq 10^7$ to 10^9 atoms). Such calculations can nevertheless provide information on a very limited part of the protein, for instance inside the filter [47–51], to interpret possible mechanisms for the Na^+/K^+ selectivity.

At the opposite side, the continuum electrostatics methodologies avoid the atomic description of the system by replacing the discrete matter by dielectric continua with rigid boundaries. While such calculations are simple and practical to analyze the influence of the protein electric field on the ions' behavior, they appear to be rather artificial and totally unadapted to the description of concerted motions of ions and protein walls [52].

The most used methods are Molecular Dynamics (MD) and Brownian Dynamics (BD), which are very complementary as much in time scale as in size scale. MD allows simulations to be performed by including reasonably large numbers of atoms ($\approx 10^5$) when classical force fields (AMBER [53], CHARMM [54], GROMACS [55], NAMD [56]) are used. Free energies, protein relaxation and diffusion coefficients can be determined, even if this method is very expensive in terms of computational time, but it cannot include physical times longer than a few tens of nanoseconds. This weakness of the MD is the strength of the BD since microsecond scale can be easily reached to simulate the whole ion diffusion in the channel. The counterpart is the poor description of the protein in terms of continuum and the use of parameters that should be calculated independently. MD can nevertheless provide parameters such as diffusion coefficients and information on the modification of the electric field due to the channel distortion, and, in this sense, both simulation methods are complementary.

Because continuum approaches also including BD simulations are too much parameterized, thus introducing inaccuracies in the results, and because MD simulations are very restrictive in terms of the system size and also dependent on the classical force field used to describe electrical properties of the protein, no direct path perfectly exists to analyze the ion permeation of the membrane. Therefore, aside from these conventional methodologies, some physical and numerical ansatzs have been used to reduce computational times and, sometimes, extend the validity limits of the method. As a first example, octane, which is known to have roughly the same dielectric properties as the lipidic bilayer but a much lower viscosity, can be substituted to describe the membrane surrounding the protein in order to favor relaxations, and more generally motions, of protein atoms [57]. As a second example, to

artificially decrease gating time, constraints can be applied to various parts of the pore. As a third example, the cytoplasmic part containing the N and C residues is generally disregarded, at least in the gating process. Such approximations, although sometimes unavoidable in practice, lay some doubts on the accuracy of the calculations.

The results presented in this paper were obtained from MD simulations using AMBER 8 suite of programs [53]. We used a 75 Å side periodic simulation box, containing nearly 6,300 atoms, forming the membrane part of the protein (pdb 1K4C), embedded in a 29 Å thickness octane slab. The extra and intracellular media are constituted by more than 6,200 TIP3P water molecules, and around 30 ions and counterions, forming two slabs of 22 Å of thickness. Simulations were conducted at constant temperature T (300 K) and atom number N. Quantum calculations on restrained part of the channel were performed by using Gaussian03 [58], at the Hartree-Fock 6–31G(*d*) level of theory.

Conductance and gating

While the diffusion model based on an ionic single file is now well-admitted [2, 27, 34, 59–61], it is not known whether the general structure of the protein controls the conductance or whether this latter is limited at one or several locations in the channel. As discussed above, since a complete description of the pore properties is not computationally possible, most of the studies have been devoted to a selected part of the channel. Moreover, permeation through the channel is gated and, at a minimum, one gate should open or close on command to regulate the ion flux. Here again, no complete information on the gating mechanism exists. In particular, no clear answer is, up to now, given to the following questions:

- What are the atomic structures of the open against closed states of the protein? And what are the consequences of opening on the ion properties?
- Are there one, two or even several activation gates which act in an independent way or being strongly correlated? Which pore part(s) finally control(s) the ion diffusion?
- What is the role of water in the ion conduction mechanism?

Attempts to give partial explanations to these features are available in the literature via studies focused on various levels of the pore structure, with different methodologies presented in the following sections of the paper.

The opening mechanism

When the crystallized structure of the KcsA was first published, paramagnetic spin resonance studies, associated with pH-dependence analysis indicated that it corresponds to a close conduction state and that the transmembrane helices forming the intracellular pore can move away from the channel axis to induce gating [37, 62]. A series of studies have thus been conducted, using MD and BD simulations, to interpret the influence of conductance with pore opening [57, 63–66]. A preliminary work in all these studies was to create a more or less stable open state of the pore. This is possible by using several methodologies. Steered MD has been independently performed by two groups [64, 65], by artificially stabilizing the aperture at the desired configuration, using a repulsive cylinder inside the pore or by placing a Van der Waals balloon at the intracellular mouth of the channel and gradually inflating and displacing it. The KcsA gating was also studied by a normal mode analysis (NMA), by considering mainly the lowest frequency modes responsible for the largest displacements [67]. A similar approach, on the basis of collective motion analysis named PCA (principal component analysis), was proposed to extract the functionally relevant motions of the protein from the simulation noise due to atomic fluctuations [68]. Homology with Ca^{+}-gated channel MthK and voltage-dependent channel KvAP has also been extensively discussed; these channels being assumed to nicely represent the open conformation of KcsA [3, 4, 7, 29, 37, 41]. However, we can wonder whether the open state of MthK mimics in a convenient way the open state of KcsA.

Targeted MD have been recently developed to study, via an all-atom description, the opening of the pore [69]. Starting from the skeleton of the crystallized close state of KcsA modelled on the basis of x-rays experiments, large constraints were applied to ions and water molecules in the filter to avoid their escape and thus to keep them at their electrostatic sites. In contrast, C_α carbon atoms of transmembrane helices M_1 and M_2 were progressively stretched to new positions, some of them being derived from an open state issued from EPR experiments (pdb 1JQ1) [70], while the others were free to move consistently with the surrounding structure. The results of these simulations have shown that the external transmembrane M_1 was not significantly perturbed by the gating mechanism. In contrast, the inner transmembrane helices M_2 moved significantly to open the channel, with root mean square displacements around 1.25 Å instead of 0.5 Å for the closed state. It may be noted that these values are only averages over all C_α atoms of M_2 helices and they do not give information on the detail of the opening, in particular what part of these helices in the cavity are mainly concerned with the gating, and how and where the pore opens first.

The study of distance variation between homoresidues in the tetrameric backbone located at the bottom of the cavity and in the intracellular medium demonstrates that channel opening proceeds as a zip [71]. Indeed, the narrowest part

of the tepee forming the gate does not open first: the opening initiates from residues located at the inner end of M_2 helices, i.e. located in the cytoplasm, with an abrupt increase of the distance between His124 and 227 of about 15 Å when submitted to the restraint. Once this increase has been stimulated, it is sufficient to open the gate zone (around Leu110 and 213) by about 4 Å, with an asymmetrical behavior for the other two monomers.

In contrast, the intra-cavity part of M_2 helices does not distort significantly and a hinge point around Met96 is obtained. The subsequent question that arises is the stability of the open state. By releasing the constraints, an asymmetric relaxation of the C termini in the M_2 helices proceeds, indicating that two monomers get closer (His-His distance equal to 19 Å) whereas the other two monomers stay roughly open (His-His distance equal to 30 Å). In the gate region, although the distance between homoresidues Leu-Leu decreases, the conformation still corresponds rather to the open state than to the closed one (Fig. 4).

The analysis of the low-frequency vibration modes of the protein has revealed that M_1 and M_2 transmembrane helices undergo totally concerted tilting and rotational motions [67]. However, M_1 motions do not directly modulate the size of the cavity, in contrast with M_2 helices. Two pivots were identified near Met96 and Thr107. The first pivot divides the KcsA subunit into a highly rigid part including the small-pore helix and the TVGYG sequence of the filter, and a much more flexible portion containing M_1 and M_2 helices (Fig. 4). The second pivot allows the swinging motion of M_2 helices and leads to an enlargement of the intracellular gate without loosening up the integrity of the protein structure. Such results are comparable with those issued from the targeted MD, which give hinge points at Met96 and Leu110 (closed to Thr107) although they do not take into account the influence, probably dominant, of the cytoplasmic part of the M_2 helix ends (Fig. 3).

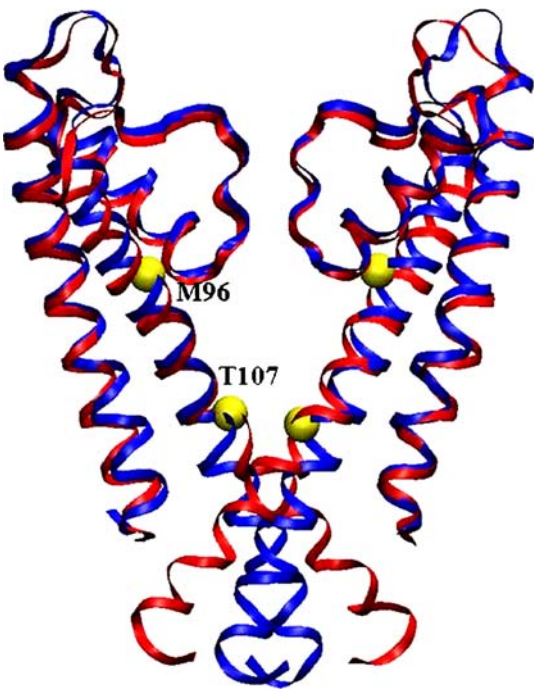

Fig. 4 Superimposed structures of the closed (*blue*) and open states (*red*) of the channel. *Yellow spheres* correspond to hinge points (Met96 and thr107). Note the strong deformation of the terminal M_2 helices

It may be noted that the magnitude of the KcsA pore opening found in the targeted simulation is much smaller than expected from the MthK homology, although the Met96 hinge point corresponds for the two channels. However, this opening is sufficient to allow for large displacements of the K^+ ions and thus to favor diffusion, as demonstrated in BD simulations [63].

The cavity

As a consequence of the large deformation of the M_2 helices, the cavity they form is the most influenced part of the pore during the opening. This inverted tepee-like structure forming a hydrophobic cavity filled by 20–40 water molecules is known to receive a well-hydrated K^+ ion. Due to its hydrophobicity and to the strong electric field it generates via the COOH termini of the α-helices of the pore, the cavity contributes to stabilize the ions in the channel and to focus K_{cav} along the pore axis, favoring the throughput. The cavity properties have thus been associated to the gating mechanism which was at the basis of the channel conductance.

When the M_2 helices move away, the volume of the bottom part of the cavity near the Leu110 increases by 15% with respect to the closed state, and the volume of the intracellular gate region increases by a factor 8 [65, 71]. This structural change in the M_2 helices conformation is followed by drastic modifications in the electrostatic field created by the protein on the K_{cav} ion (Fig. 5). Indeed, in the closed state, the cation experiences a positive field everywhere along the cavity axis, which tends to stabilize it at the top of the cavity. When the gate opens, the influence of the electric field becomes less significant, with a loss in the ion stability inside the cavity. At the cavity bottom, i.e. at the gate, the electric field displays two opposite peaks (one negative and one positive) in the closed state, which prevent the ion diffusion in both directions. On the contrary, this field remains positive in the open state and tends to favor the diffusion toward the filter. These effects are then magnified by the presence of water.

Indeed, water plays crucial structural and dynamical roles in the cavity [72, 73]. In the closed state of the pore, the S_{cav} site is revealed by the organization of the confined water molecules inside the hydrophobic cavity, while the

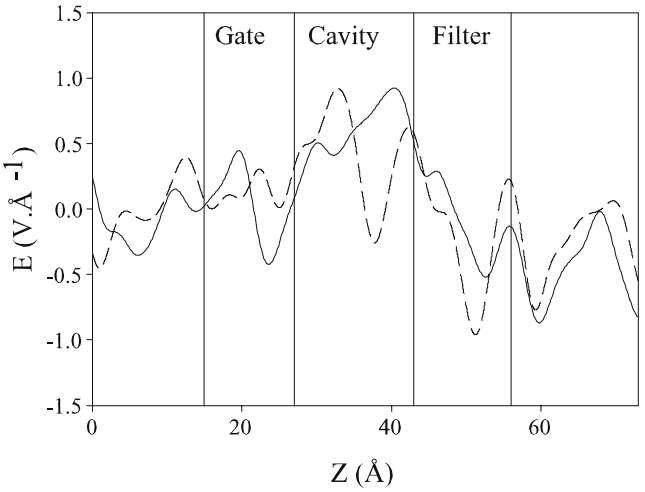

Fig. 5 Behavior of the electric field versus the z position of the ion along the channel axis for the closed (*full curve*) and open (*dashed curve*) states of the channel

electric field of the protein itself does not create such a stable site. Statistically, this site is closer to the filter mouth than to the middle of the cavity, while the water molecules tend to bolster the K_{cav} ion in this conformation by creating an electric dipole moment directed toward the gate (Fig. 6a). In the open state, the K_{cav} ion tends to move toward the gate, being surrounded by the water molecules which create a dipole oriented toward the filter (Fig. 6b). The change of electric field promoted by the water molecules in the cavity during the opening appears therefore drastic and should influence the ionic conduction. Homology studies have corroborated the fact that a cation located in the cavity is less stable in the open state than in the closed state, due to a high dielectric environment in the vicinity of the cavity ion [37].

Water also appears as a major dynamical element in the cavity due to its high mobility. Opening the gate induces a large mobility of water molecules from the intracellular to the cavity and vice-versa. The number of water molecules in the open cavity fluctuates slightly around 38 instead of 32 in the closed state (Fig. 7). It may be noted in addition that the molecules can exit or enter the cavity, and although the total number is conserved, a third of these molecules was changed in 1 nanosecond. This is a contrasted situation with the closed state, in which the water molecules cannot escape the cavity. The water molecules are strongly correlated to the K_{cav} ion motions in order to create a hydration sphere (Fig. 8), but this correlation does not prevent water molecules from moving in the cavity by creating/breaking hydrogen bonds, and even escaping from their hydration sphere to leave the cavity in the open state. There are in fact permanent exchanges of water molecules in the solvation sphere of the K_{cav} ion [73].

Since gating of the KcsA is activated by a drop in pH, *ab initio* calculations have been conducted to study the role of

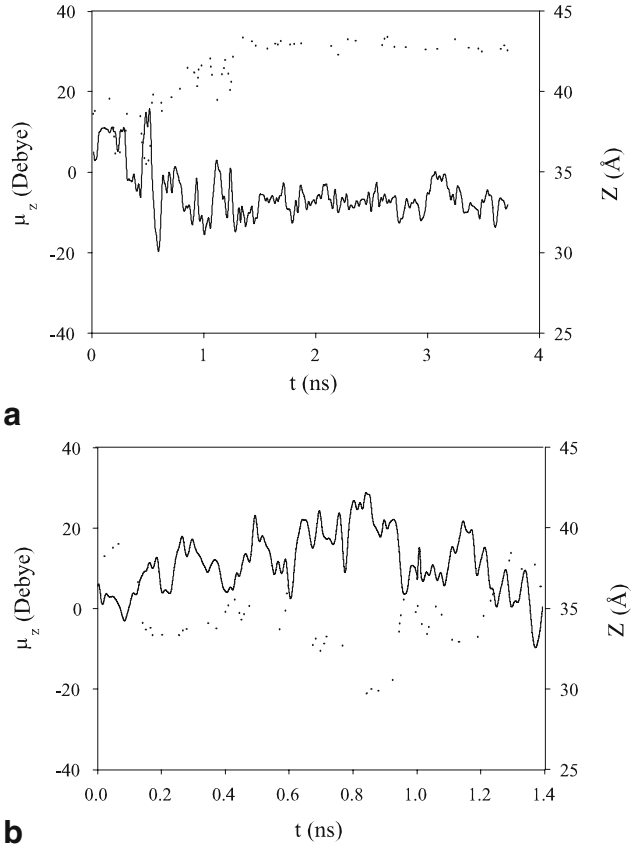

Fig. 6 Behavior of the component μ_z of the dipole moment created by the water molecules inside the cavity (*full curve*) as a function of the simulation time. The corresponding position of K_{cav} along the z axis inside the cavity is drawn versus the time (*dotted curve*) for closed (**a**) and open (**b**) states of the channel

water at bundle crossing of M_2 helices in the cavity. Results suggest that an H_5O_2 group, partially charged, would connect or disconnect glutamate residues in the gating

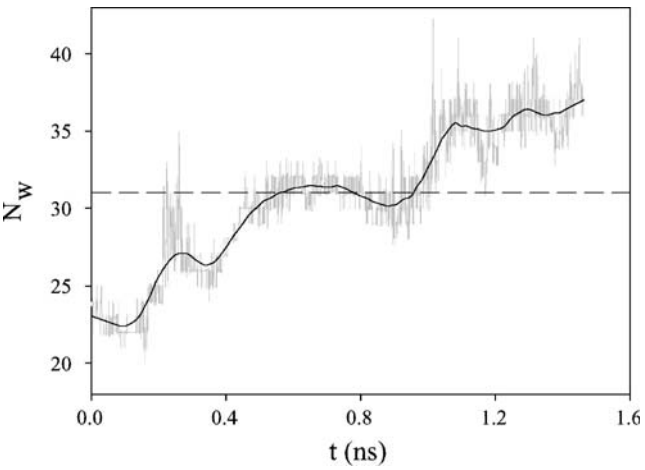

Fig. 7 Number of water molecules in the cavity versus the simulation time for closed (*dashed line*) and open (*full curve*) channel. The curve represents smoothed data of the grey curve including the instantaneous variations of the number of molecules. In the closed state this number is constant, there is no exchange of water with the intracellular medium, whereas it increases during the opening of the channel

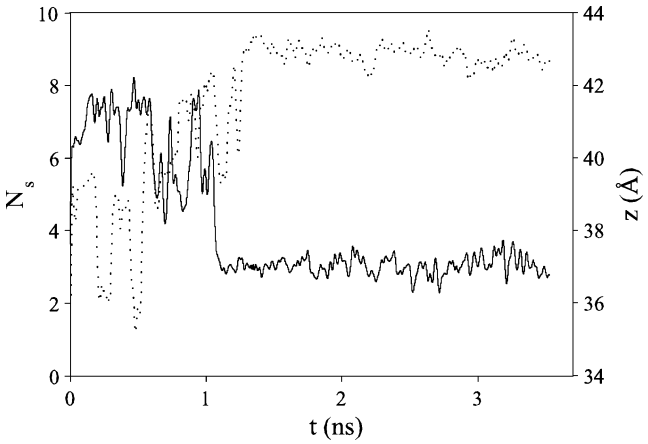

Fig. 8 Behavior of the number of water molecules in the first hydration shell (*dotted curve*) versus the simulation time and of the corresponding position of the ion along the z axis (*full curve*) in the closed state

region, depending on the net charge of the four residues (respectively −2e or −1e, where e is the electronic charge). The arrival of a proton responsible for the change of residue charge would in fact lead to weak H-bonds insufficient to hold the gate closed. Such a mechanism could be at the origin of the gating process [74, 75]. In fact, recent publications have shown that two gates should open simultaneously to permit the conduction of KcsA. The main gate formed by the bundle crossing of the transmembrane M_2 helices at the innermost part of the cavity is open by a pH decrease [62] as indicated before, while the second gate, connected to destabilizing interactions between residues in P loop (mainly Asp80 and GLu71), is promoted by Glu71 that acts as a gating charge depending on variations of the membrane field [9, 10, 76, 77].

The filter

During the opening of the pore by targeted MD, the C_α carbon atoms of the filter do not show strong deviations from their equilibrium position since the root mean square displacement does not exceed 0.2 Å, while the protein displacement is clearly much important (around 1.3 Å) [69]. Moreover, a drastic event such as the sudden switch from NVT to NPT distribution (where the constraint on the volume V of the simulation box is released to a process at constant pressure P) does not perturb the filter backbone, even if the filter plays a crucial role in the conductance control.

The filter is the best known region of the pore at the atomic level from x-rays experiments. This narrowest part of the channel, formed by residues corresponding to the sequence TVGYG, creates through carbonyl oxygen atoms ideal solvation sites for nearly dehydrated K^+ ions. The rate-limiting step in the ion conduction mechanism, which was elaborated many years ago [43] and then adapted according to improvements in the knowledge of the protein structure [2], is the concept of translocation. This translocation was then described as totally concerted barrierless motions of dehydrated ions in single file which recover, via the sites formed by carbonyls, solvated states [59, 60].

However, since x-rays data are static, performed at 77 K, and for the closed state of the channel, simulations have been extensively developed to reproduce channel conditions at 300 K, including protein motions and distortions correlated with ion diffusion. Simulations generally start from initial atomic coordinates obtained by embedding the protein structure in a pre-equilibrated membrane and then adding water molecules and ions at 300 K. When applied to the filter part of the channel, they have corroborated that permeation occurs via concerted single-file motion of K^+ and water molecules. They have furthermore shown that the innermost walls of the filter undergo small changes, with the oxygen atoms of the carbonyls lining the pore moving as the ions switch along the sites. The correlated motions of carbonyls and ions, indicating that the filter should be reasonably flexible, have been invoked to explain the rapid ion flux across the pore [21, 33, 78]. Conformational dynamics of the filter has also been considered for occasional distortions implying peptide bond flips, where some carbonyls change their orientations. The results suggest that such distortions, which can be controlled by pH change [9], could have an influence on the permeation mechanism. Indeed as shown in crystallized structure of KcsA, high K^+ concentrations lead to an equilibrated, rigid, structure with well-organized carbonyl groups, while low K^+ concentrations tend to destabilize carbonyl arrangement (CO flips are observed at the Valine level) [38]. Models have been proposed to explain ion kinetics across the filter by stating that diffusion proceeds via a concerted switch of K^+ ions at the four filter sites S_1-S_4 [79–81].

At present, the MD simulations tend to prove that diffusion occurs via a knock-on process. This mechanism consists in the alternation of two or three ions occupation states in the filter [27, 43, 61]. Most of the time there are only two ions in the filter, which occupy alternately the sites S_1-S_3 or S_2-S_4. While the sites S_1-S_3 are filled, it is possible for an ion located in the cavity to enter the S_4 site of the filter leading to a sudden contraction of the file and to the displacement of ions in sites S_0 and S_2. This transition state S_0-S_2-S_4 is followed by a rapid dissociation and the departure of the S_0 ion to the extracellular side. The efficiency of such a transition has been estimated using molecular dynamics simulations by considering concerted fluctuations of the ion positions in the file and cavity. It was shown in a recent paper that such a process occurs each nanosecond, a value that could be compared to the experimental estimation of 10^8 diffusing ions per nanosecond [82].

The role of water molecules confined in the filter, the number of which is in fact restricted to the two molecules

placed in alternation with the two K^+ ions [38, 45], has long been limited to a screening of the repulsive interactions between ions and to a completion of the solvation of the K^+ ions in the filter. In fact, in single file transport, it has been shown that water molecules are more than just spacer molecules. Molecular dynamics simulations supported by electrostatic calculations have shown that water molecules act as a structural element for the K^+ ions inside the filter. Indeed, water tends to enhance the depth of the wells occupied by the K^+ ions, which themselves stabilize the protein, and creates a new well in the cavity (Fig. 9) [83].

Moreover, water molecules are constrained to move with the K^+ ions through the filter, their motions being strongly correlated [83, 84]. The couple K_0-W_1 corresponding to a K^+ ion in site S_0 and a water molecule in site S_1 move in a concerted way, as does the couple K_4-W_3, when an event tends to modify the constraints imposed to the protein (Fig. 10). These concerted motions are consistent in magnitude as well as in the slope of the displacement versus time (velocity drift). A strong correlation between the couples K-W (Fig. 11) and the oxygen atoms of the carbonyl groups closer to these couples is also observed. This is the case for K_0-W_1 and the oxygen of Tyr78 in a monomer, which exhibit displacements with nearly the same amplitude (Fig. 10a). It may however be noted that the two couples K_0-W_1 and K_4-W_3 appear to be in phase opposition under the switch NVT/NPT, instead to be in phase concerted.

Water molecules can also play a significant role at the two mouths of the filter. On the extracellular side of the channel, the K^+ ion located in the site S_0 has been detected in the 2.0 Å resolution x-rays structure to be rather fully hydrated [38]. In contrast, simulations have shown that this ion is only partially coordinated to water molecules and

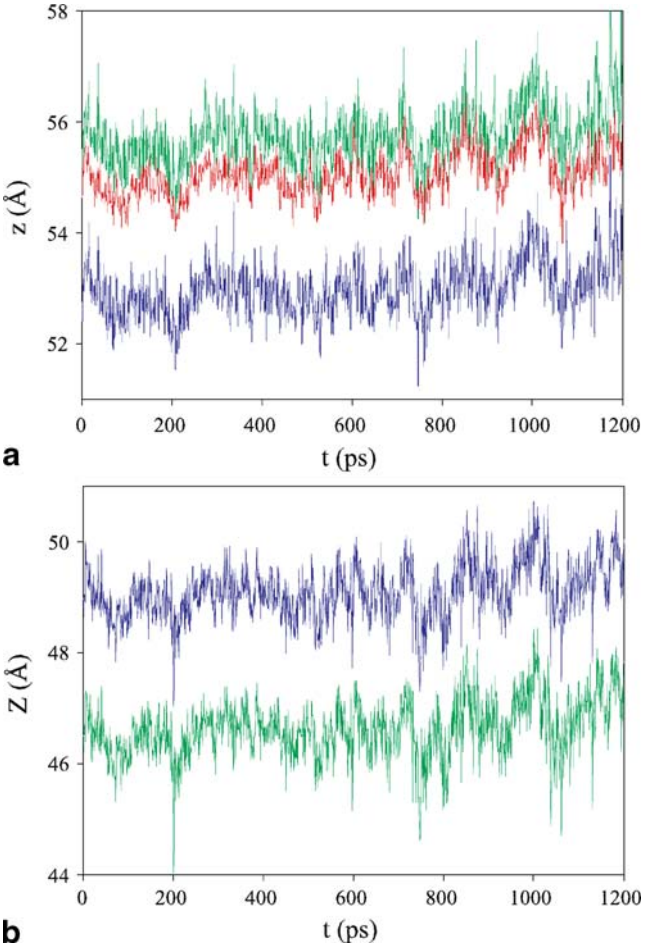

Fig. 10 Time evolution of the position of various atoms in the filter. **a** K_0 ion (*green curve*), W_1 water (*blue*) and mean positions of carbonyl oxygen atoms of the four Tyr78 (*red*). **b** K_4 ion (*green*) and W_3 water (*blue*)

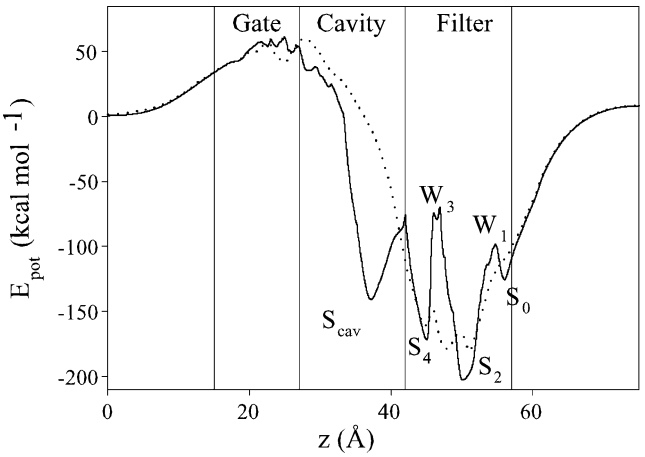

Fig. 9 Behavior of the potential energy due to the protein experienced by a single K^+ ion moving along the channel (*dotted curve*) compared to the potential energy of the same ion when water is included in the channel (*full curve*). Sites S_1 and S_3 are filled by water while S_0, S_2 and S_4 correspond to the ion location

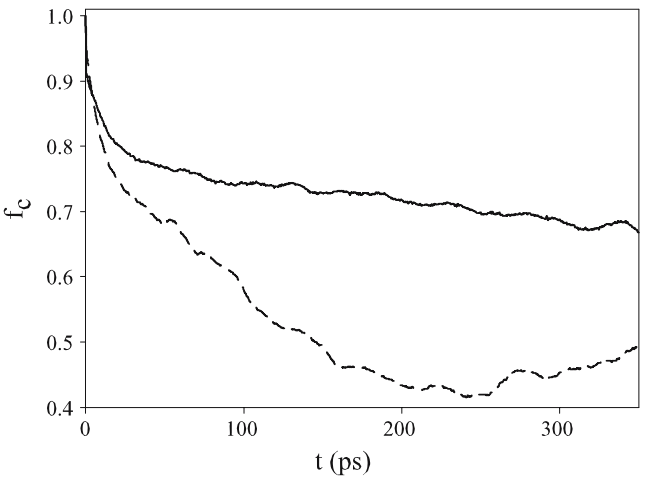

Fig. 11 Time correlation function for the couples K_0-W_1 (*dashed curve*) and K_4-W_3 (*full curve*). Note the difference in the correlation of the two couples due to the fact that K_0 ion tends to exit the filter while K_4 prefers to enter the filter

transiently solvated by the carbonyl oxygen atoms of Tyr78 [27, 35, 46]. At the inner mouth of the filter, i.e. close to the cavity, simulations found two adjacent sites for K_4 ion, which allow its back and forth motions at the filter entry. The K_4 ion is also very partially hydrated and solvated by the carbonyl oxygen atoms of Thr75. From a structural point of view, the surrounding water molecules act thus by revealing S_0 and S_4 sites (Fig. 9).

Moreover, entry/exit of these ions in the inner/outer mouths of the filter have been suggested by experiments and simulations to be a key determinant of conductance magnitude. Two reasons have been invoked. The first is based on hydration/dehydration energy required to exit/enter the filter [16, 23, 85]. The second relies on the structural confinement of water. Due to geometrical confinements in the selectivity filter, (1) liquid–vapor oscillations occur where the file of molecules embedded in the channel (the liquid) cooperatively exits the channel, leaving behind a near vacuum (the vapor) [86, 87], and (2) dielectric properties of confined water are distant from those of the bulk, with a permitivity constant that can be reduced by a factor 2, and the corresponding electric fields are dramatically changed [88, 89]. This second argument is reinforced by the hydrophobic character of the inner and outer mouths of the filter. This tends to stabilize H-bonds between water molecules over times which can be increased by a factor 10. As a result, proton transfer is favored and this latter process can promote specific bindings at filter mouths influencing the conductance.

The cytoplasmic region

Little attention has been paid to C and N terminal domains of K^+ channel in cytoplasm, probably due to a lack of understanding of structural relationship of these two domains to the rest of the channel. While N termini are probably responsible for the anchoring of channel to membrane, C termini form with transmembrane helices M_2 a large water filled cavity which appears as a natural path for ion permeation (Fig. 3) [5]. The few simulations available to date, to our knowledge, have demonstrated that these domains have no direct effect on ion conduction in KcsA but that they could influence the gating, through in particular the electrostatic field they create under local rearrangements [90, 91].

Conductance and selectivity

Since transmembrane ion channels partition the exterior from the interior of the cell in order to maintain, in particular, the proper ionic gradient in the cell, it must be highly selective, allowing some ions to pass while blocking other species. To discriminate between the different ions with different charge values, the protein electrostatic potential must analyze the ion charge to decide whether the ion can cross or not the membrane. In the KcsA channel, the selectivity is ensured by charged carbonyl oxygen atoms that attract monovalent cations and repel anions [92, 93]. However, for monovalent cations with the same charge, such as K^+ and Na^+, the selectivity appears to be a more subtle phenomenon. Most studies on the Na^+ versus K^+ selectivity of the KcsA channel have been devoted to the filter [18, 20, 21, 94], which is recognized as the dominant part of the pore selectivity, but the other zones can also promote selectivity through their specific properties [95, 96]. In analogy with what has been done for the gating, we will thus explore the different parts of the pore to discuss selectivity.

The filter

The selectivity filter has received considerable experimental attention since the pioneering studies by Chandler et al. [14], Hille [17] and Armstrong [1]. To interpret the selectivity of this narrow part of the pore, they postulated that Na^+ was too small to fit well in the coordination cages provided by the K channel, in comparison with the water molecules forming the hydration sphere of the cation. This model was then renewed when the crystallized structure of KcsA was published [2]. It was shown that eight carbonyl oxygen atoms in the filter play the role of water in hydration sphere for a cation K^+ in each site S_1, S_2 and S_3. The preference for K^+ over Na^+ was thus explained as the result of a nearly perfect compensation of the K^+ dehydration by the channel carbonyl solvation, while such compensation was not possible for a smaller ion, such as Na^+ [18, 22] (Fig. 12).

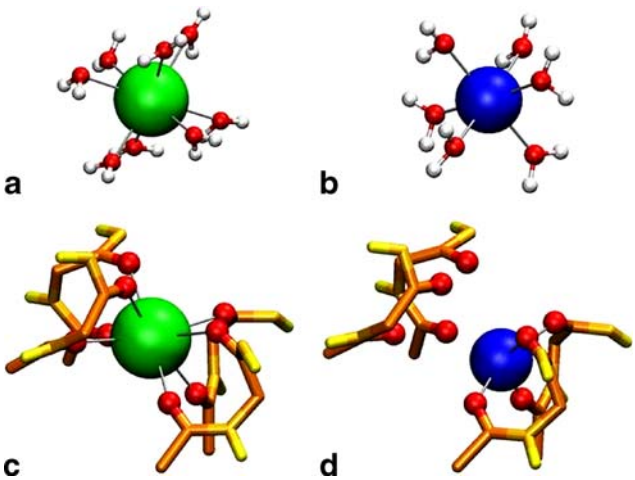

Fig. 12 Geometry of the first hydration shell of ions in bulk water, octahedral geometry for potassium (**a**) and tetrahedral one for sodium (**b**). First solvation shell of potassium ion (**c**) and sodium ion (**d**) in the site S_2 of the filter

In some papers [21, 78], and in particular in a more recent one [97], it was nevertheless argued that the size difference between K^+ and Na^+ radii (0.38 Å) is too small to be retained as an argument to explain selectivity if we consider that proteins are "soft materials displaying structural flexibility". In particular, it was shown, in a simple model including the eight carbonyl groups, that the C=O dipoles are very dynamic, and their electrostatic properties, rather than their structural conformation, control the cation selectivity by increasing or decreasing the resulting dipole moments of the protein walls. In contrast, experiments conducted on Na^+/K^+ selectivity of NaK channel, which shares high sequence homology and similar structure with the KcsA channel, tend to demonstrate that the electrostatic repulsion between carbonyls would not explain the selectivity [98]. From these results, the size-selectivity through geometric constraints was privileged. However, recent additional calculations based on the dynamical role of the C=O dipoles have shown that thermodynamic exclusion of Na^+ relative to K^+ was due to the scarcity of favorable binding configurations for Na^+ compared to K^+ in the filter. The enhanced fluctuations of the binding energy for the smaller cation could thus be at the origin of this selectivity [99].

The incidence on selectivity of polarizations and charge transfers between the cations in the filter has recently been discussed. Previous DFT (Density Functional Theory) calculations showed that, during the translocation process from one site to another one in the filter, the K^+ ion significantly polarizes its ligands, the carbonyl groups and the neighboring water molecule(s) [47, 100]. These results were contradicted by other authors who compared *ab initio* Hartree-Fock and DFT calculations of partial charge for K^+ ion in the filter, from a study of the electrostatic potential experienced by the cation [48, 51]. This comparison suggested that the DFT method overemphasizes the importance of polarization. The electronic structure of the selectivity filter polarized by the electrostatic field of the environment was investigated using DFT and QM/MM methods. It was shown that the carbonyl groups were largely polarized and that a charge transfer took place between the backbone and the cations, with a more pronounced effect for Na^+ than for K^+ in the cation sites explored.

A more extensive analysis of the incidence of partial charge on the pore selectivity has been carried out in our group. In a first paper [49], *ab initio* calculations were performed to calculate the atomic charges in the selectivity filter according to Merz-Kollman-Singh (MKS) scheme [101, 102]. Emphasis was mainly devoted to the determination of the charges of (1) the oxygen atoms in the two water molecules, (2) the two K^+ ions in the filter, (3) the nitrogen, the carbon and the oxygen atoms in peptide bonds and (4) the carbon and the oxygen atoms of the CHOH part of the Thr74 lateral chain. Significant decreases of the K^+ charges in sites S_2 and S_4 up to about 0.31 e were observed, while the charges of oxygen in water molecules decrease by 0.20 to 0.25. Similar changes were calculated for the atoms belonging to peptide bonds and hydroxyl groups of Threonine, with a strong dependence on the proximity with a given site (S_2 or S_4). These results, obtained for K^+ only, needed to be extended to Na^+. This was done in a second paper [50], using two methods for charge partitioning from the knowledge of the electrostatic potential. These two methods (MKS and HR [103]) allowed us to be confident that determination of partial charges was not too dependent on the choice of the partitioning. Four situations were then considered, which correspond to water–cation sequences in S_1 to S_4 sites of the filter. The WKWK sequence, for which the two water molecules are located in S_1 and S_3 sites while K^+ ions occupy the other two sites, could be compared with situations for which one or two sodium ions are substituted to potassium. The results showed, in both charge partitioning methods, that the mean partial charge for K^+ is always much more affected by charge transfer process, with a value which is smaller by 25% than the electronic charge, instead of less than 10% for Na^+ in the S_2 and S_4 sites. The values of the partial charges depend on the position of the two cations species in the sequence, with a charge decrease which is more pronounced in S_4 site than in S_2 for both K^+ and Na^+. The corresponding partial charges on the oxygen atom of water molecules in S_1 and S_3 sites also significantly decreased, up to 30% for S_1, while this change was much smaller for S_3.

In terms of electrostatic potential experienced by any cation in a given sequence, the charge transfer process did not change the overall shape of the potential curves, indicating that the four sites were in general well defined. In contrast, the depth of the wells connected to those four sites was shown to depend on the cation species in the sequence. In the calculations, it was found that the energy difference in the wells can reach 40 kcal mol^{-1} when a Na^+ cation is substituted to a K^+ one. This value is dramatically larger (by a factor of 4) than the value calculated by considering the electronic charge for the two cations, and it could be at the origin of the K^+/Na^+ selectivity of the KcsA channel. Unfortunately, this value led to a selectivity ratio unrealistically large, using the model of Nelson [79].

The main problem to estimate the selectivity in this charge partitioning method is the use of a constant partial charge for the cation along the filter and a common structure of the protein for the two species. Indeed, the charge should depend on the position of the cations in the filter and on the possible distortion of the filter conformation by changing K^+ to Na^+, particularly regarding the orientation of carbonyl groups. This variation has been

taken into account for a more accurate estimation of the selectivity ratio P_{K^+}/P_{Na^+} in a third paper.

We have performed targeted molecular dynamics simulations to mimic the diffusion of a water-cation sequence from sites S_4 to S_0. The sequence $K_0W_1K_2W_3K_4$ was moved along the filter to reach the $W_0K_1W_2K_3W_4$ occupation, which was sufficient to determine the partial charges for each site (Fig. 13a). A similar procedure was then applied to the sequence containing one Na^+, which was moved in the two directions from S_2 to S_4 or S_2 to S_0 in order to explore every site (Fig. 13b). The quasi continuum behavior of the Na^+ and K^+ charges in the sequences moving along the filter was then analyzed, showing that these partial charges fluctuate significantly when the ion transits from a given site to another one. Including the filter distortion, disregarding in a first step the charge fluctuations and considering only a mean behavior that reflects the value of the partial charge in the five sites (S_0-S_4), we see (Fig. 14) that the Na^+ charge is equal to the electronic charge in site S_0 and decreases by less than 8% in site S_1. For K^+, while the charge is close to the electronic charge in S_0 and S_4, it decreases by 16% for S_2. From these results, the calculated selectivity ratio P_{K^+}/P_{Na^+} was estimated to be around 10^6, a value which appears closer to the experimental value equal to 10^4. The energy difference between Na^+ and K^+ now ranges between 6 and 12 kcal mol^{-1} (Fig. 15). These values are still too high by a factor of 2 in order to explain the experimental data. In fact, such values should be corrected to account for the entropic contribution, i.e. by calculating the free energy difference within the transition state theory [24–27] and not the potential energy difference. Such a calculation is in progress. However, without anticipating the results, it may be noted that inclusion of this entropic term should significantly reduce this difference and probably provide a better agreement with experiments.

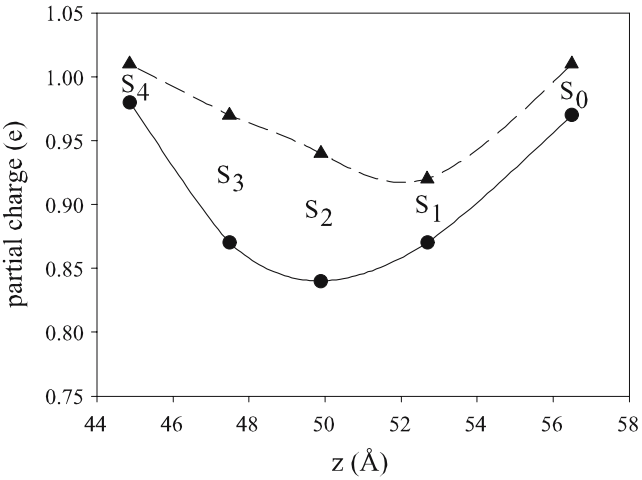

Fig. 14 Mean partial charge of K^+ (*full curve*) and Na^+ (*dashed curve*) ions along the axis of the filter

The polarization and charge transfer processes are thus clearly phenomena that must be accounted for to interpret conductance and selectivity of KcsA channel. In the filter, these processes are magnified due to atom confinement, and we can also wonder whether they could explain the cavity selectivity, which is discussed in the following section. An accurate calculation of the selectivity ratio should in fact include a set of selectivity processes involving the filter, its inner and outer mouths and the cavity. In contrast, the selective role of the cytoplasmic region of the protein is not known. In the very scarce studies of this protein part, it seems to serve rather as a receptor of cytoplasmic activators [5, 91, 92]. However, the fact that large electrostatic fields are generated by this part could suggest other influences.

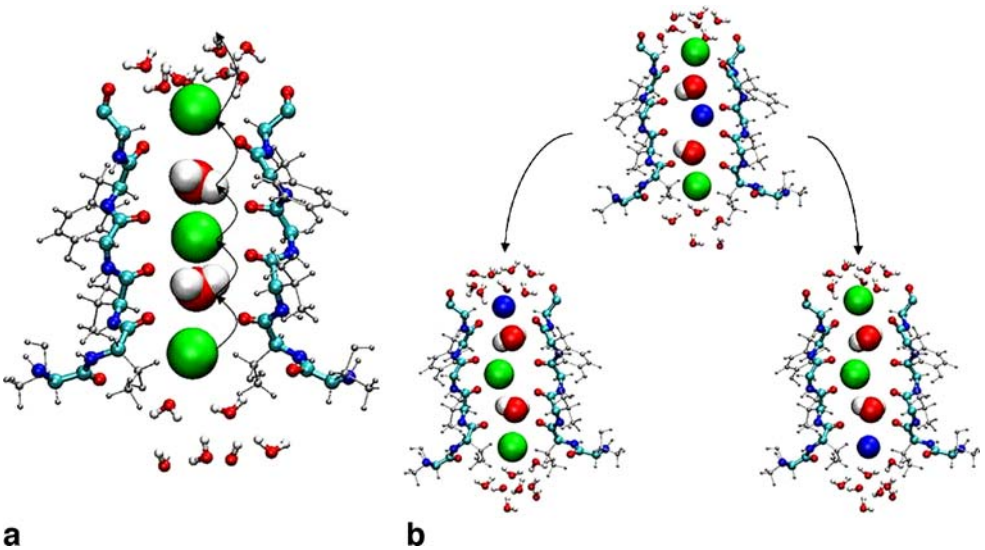

Fig. 13 **a** Diffusion of the KWKWK sequence along the filter. **b** Diffusion of the Na^+ ion (*blue sphere*) in the sequence, toward the outer part of filter (*left*) and toward the inner part (*right*)

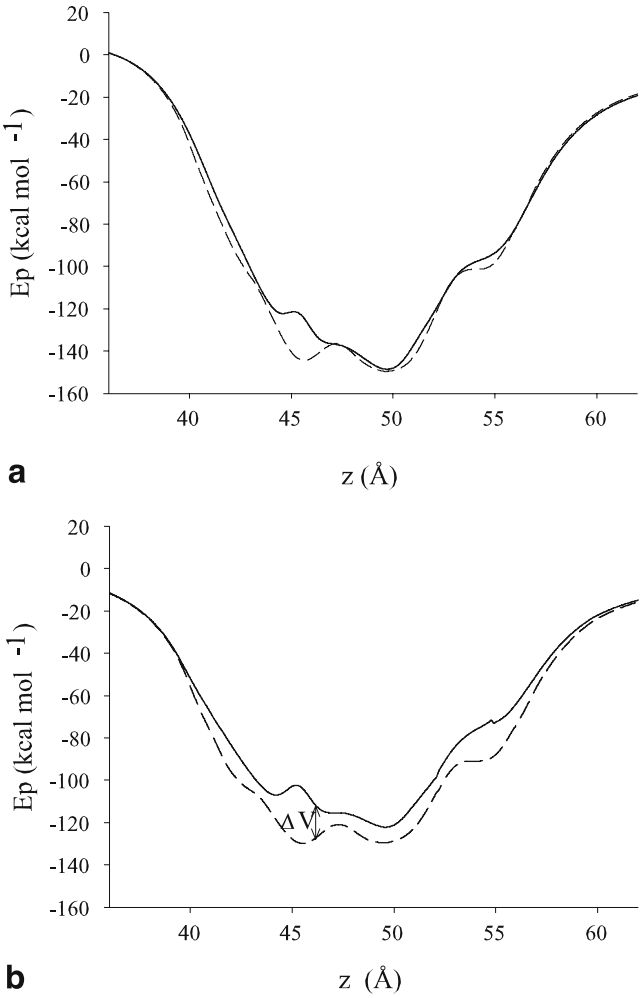

Fig. 15 Potential energy experienced by K^+ (*full curve*) and Na^+ (*dashed curve*) along the filter using either the standard charges (**a**) or the partial charges (**b**) for ions and filter atoms. ΔV characterizes the energy difference which is used to determine the selectivity ratio (see text)

The outer and inner mouths of the filter

Aside from the binding site S_0 located on the extracellular side of the channel, which corresponds to the partial hydration by three to four water molecules and to the additional coordination with carbonyl oxygen atoms of Tyr78 of the K^+ ion occupying this site, there exists another site S_{ext} in the outer mouth of the filter, for which the ion is more hydrated [27]. Crystallographic data have demonstrated the existence of these two different positions which could represent the transition sites corresponding to dehydration/rehydration, as a cation enters/exits the filter. Since this mechanism is about 18 kcal mol^{-1} more energetic for Na^+ ion than for K^+ ion in bulk water, it could be invoked to explain the selectivity ratio K^+/Na^+. However, the ability of the cation to dehydrate or rehydrate at a specific location should also depend on an intimate interaction with the protein. No calculations are presently available to estimate this hydration energy of the two cations in a confined water medium submitted to the influence of strong electrostatic field of the protein.

Moreover, experiments conducted on voltage-gated K^+ channels have shown that protonated Histidine influences selectivity K^+/Na^+ independently of the filter [85]. In particular, mutation of this residue to neutral amino acids increases the selectivity of K^+ over Na^+, increases K^+ current through the pore and blocks Na^+. Here again, no extensive atomic scale analysis of this pore region has been performed.

Although the outer and inner mouths of the filter do not display symmetrical structures, it can be noted that the cations seem to occupy two positions at the inner mouth of the filter. These two positions, which are not discriminated in terms of sites since they are labelled under the same name S_4, correspond to situations where the cation is partially hydrated and partially coordinated with carbonyls (the outer position in the filter) and where cations are nearly dehydrated and mainly solvated by the carbonyl oxygen atoms (the inner position). This process corresponding to dehydration/solvation of the cation looks like the one which occurs at the level of sites S_0 and S_{ext} of the outer mouth.

The cavity

Although in a much smaller proportion, the cavity is known for a long time to display K^+/Na^+ selectivity. K^+ in the S_{cav} site is surrounded by eight water molecules, while the hydration structure around Na^+ is not ordered at the same level (Figs. 8 and 12). Free energy perturbation calculations for a single K^+ over Na^+ ion moving throughout the cavity up to the gate have shown energy differences ranging between 2–4 kT (1.2–2.4 kcal mol^{-1}), instead of 6–8 kT inside the filter, demonstrating the discriminatory role of the cavity [19].

Electrophysiological experiments have been performed, leading to a 5- to 7-fold preference for K^+ over Na^+, equivalent to 1 kcal mol^{-1} [95]. Using Tl^+, a monovalent cation displaying a good analogy with K^+, instead of K^+, to determine the cavity selectivity, the Tl^+/Na^+ binding affinity was estimated to be 7-fold, favoring Tl^+ over Na^+ [104]. The consistency between structural and functional data, and the additional information provided by homology with open channel, have demonstrated that this selectivity does not fundamentally depend on the open or closed state of the pore, and that it can be considered as an intrinsic property of the K^+ channels. The origin of such selectivity is not really known, and it is suggested that the electrostatic interaction between the cation and the channel, alone, cannot explain it [96].

In fact, the role of water in the cavity is probably more important than generally discussed. MD simulations have

shown that the cation occupation is different according to whether the pore is in its open or closed state [73]. Moreover, it has also been demonstrated that the hydration sphere is less structured around Na^+ than K^+ [22, 38]. These features could explain a difference in the effective charge of the two cations at the origin of the selectivity. Calculations of partial charge of the cations Na^+ and K^+ in the cavity should probably provide an answer to this remark.

Conclusion

KcsA constitutes a potassium channel that shows high conduction and selectivity of cations, as observed in permeation experiments [105]. Electropermeation experiments typically measure currents on millisecond time scales, which are clearly well beyond the possibilities offered by MD (typically around a few tens of nanoseconds), and describe conductance as a function of concentration and voltage, which cannot be satisfactorily interpreted in terms of BD.

Kinetic models based on single file ion diffusion in the filter of the channel have been proposed using stochastic processes to describe the ion configurations in terms of occupancy states and the transitions between these states. While the models differ by the description of the translocation mechanism in the filter (strongly concerted ion motions [79], knock-on mechanism based [81] on quasi-ion diffusion and ion-ion fluctuations [80]), they all agree that the permeation limiting rate corresponds to the ion entry entry/exit from the filter. This phenomenon is itself the result of association/dissociation of the ions due to the superimposition of the two effects: the electric field created by the protein at the entry/exit (a feature observed for a large class of channels [106]) of the filter and the dehydration/hydration mechanism of the cation, followed by its solvation via oxygen of carbonyls.

These models can in principle roughly explain both ion conductance and selectivity in the filter, which strongly depend on the depth of the filter well and on the hydration energy. However, these quantities themselves are sensitive to the ion, water and protein dynamics and to the configuration (closed or open state) of the channel, and they are generally considered as parameters. Therefore, only qualitative comparisons with the electrophysiological data can be made. Progress in this analysis would require a more detailed knowledge of the channel to describe the concerted dynamics of the ions and the protein in the various parts of the pore (filter, outer and inner mouths of the filter, cavity, gate and cytoplasmic region), depending on the closed and open state conformation.

Channel gating and its real influence on the pore conductance and selectivity remains an unresolved problem at the atomic scale. The very different time scales that are involved in the various processes implied in ion conductance, ranging from picoseconds for ion dynamics, nanoseconds for ion diffusion, milliseconds for ionic current to seconds for the whole gating and inactivation mechanism, prevent, furthermore, any general interpretation of the behavior of these channels in terms of numerical simulations.

Therefore, an understanding of these phenomena should be taken into account in improved versions of permeation models. These improvements would concern (1) a continuous description of the partial charges of the cations and the filter wall atoms during the ion translocation in the pore via q(z) dependence, (2) an atomic description of the water medium implying both the confinement influence and the effect of strong electrostatic forces, (3) the role of charge transfer and electric field created by the cytoplasmic termini on the rest of the protein, (4) the inclusion of the slow dynamics of the channel opening under the influence of pH changes and extra against intra cellular ion concentration variations. Moreover, (5) the activation and inactivation mechanisms in the protein, which have been evidenced using substitution residues in various voltage and pH-gated channels, could be included in an accurate theoretical interpretation of these mechanisms.

References

1. Armstrong CM (1969) J Gen Physiol 54:553–575
2. Doyle DA, Cabral JM, Pfuetzner RA, Kuo A, Gulbis JM, Cohen SL et al (1998) Science 280:69–77
3. Jiang Y, Lee A, Chen J, Cadene M, Chait BT, MacKinnon R (2002) Nature 417:515–522
4. Jiang Y, Lee A, Chen J, Cadene M, Chait BT, MacKinnon R (2002) Nature 417:523–526
5. Cortes DM, Cuello LG, Perozo E (2001) J Gen Physiol 117:165–180
6. Yellen G (2002) Nature 419:35–42
7. Jiang Y, Lee A, Chen J, Ruta V, Cadene M, Chait BT, MacKinnon R (2003) Nature 423:33–41
8. Bernèche S, Roux B (2005) Structure 13:591–600
9. Cordero-Morales JF, Cuello LG, Perozo E (2006) Nat Struct Mol Biol 13:319–322
10. Cordero-Morales JF, Cuello LG, Zhao Y, Jogini V, Cortes DM, Roux B, Perozo E (2006) Nat Struct Mol Biol 13:311–318
11. Kuruta HT, Fedida D (2006) Biophys Mol Biol 92:185–208
12. Doyle DA (2004) Trends Neurosci 27:298–302
13. Swartz KJ (2004) Nat Struct Mol Biol 11:499–502
14. Chandler WK, Meves H (1965) J Physiol 180:788–820
15. Meves H, Chandler WK (1965) J Gen Physiol 48:31–33
16. Bezanilla F, Armstrong CM (1972) J Gen Physiol 60:588–608
17. Hille B (1973) J Gen Physiol 61:669–686
18. Allen TW, Hoyles M, Kuyucak S, Chung SH (1999) Chem Phys Lett 313:358–365
19. Allen TW, Bliznyuk A, Rendell AP, Kuyucak S, Chung SH (2000) J Chem Phys 112:8191–8204
20. Biggin PC, Smith GR, Shrivastava I, Choe S, Sansom MSP (2001) Biochim Biophys Acta 1510:1–9
21. Shrivastava IH, Tieleman DP, Biggin PC, Sansom MSP (2002) Biophys J 83:633–645

22. Domene C, Sansom MSP (2003) Biophys J 85:2787–2800
23. Guidoni L, Torre V, Carloni P (1999) Biochemistry 38:8599–8604
24. Olsson MHM, Mavri J, Warshel A (2006) Philos Trans R Soc Lond B 361:1417–1432
25. Braun-Sand S, Burykin A, Tao Chu Z, Warshel A (2005) J Phys Chem B 109:583–592
26. Luzhkov VB, Åqvist J (2005) Biochim Biophys Acta 1747:109–120
27. Bernèche S, Roux B (2001) Nature 414:73–77
28. MacKinnon R (2003) FEBS Lett 555:62–65
29. Gulbis J, Doyle DA (2004) Curr Opin Struct Biol 14:440–446
30. Korn SJ, Trapani JG (2005) IEEE Trans Nanobio 4:21–33
31. Sansom MSP, Shrivastava IH, Ranatunga KM, Smith GR (2000) Trends Biochem Sci 25:368–374
32. Chung SH, Kuyucak S (2002) Biochim Biophys Acta 1565:267–286
33. Sansom MSP, Shrivastava IH, Bright JN, Tate J, Capener CE, Biggin PC (2002) Biochim Biophys Acta 1565:294–307
34. Miloshevsky GV, Jordan PC (2004) TRENDS Neurosci 27:308–314
35. Roux B (2005) Annu Rev Biophys Biomol Struct 34:153–171
36. Roux B (2002) Curr Opin Struct Biol 12:182–189
37. Jogini V, Roux B (2005) J Mol Biol 354:272–288
38. Zhou Y, Morais-Cabral JH, Kaufman A, Mackinnon R (2001) Nature 414:43–48
39. Heginbotham L, Abramson T, MacKinnon R (1992) Science 258:1152–1155
40. Heginbotham L, Lu Z, Abramson T, MacKinnon R (1994) Biophys J 66:1061–1067
41. Nimigean CM, Chappie JS, Miller C (2003) Biochemistry 42:9263–9268
42. Chapman ML, Krovetz HS, VanDongen AMJ (2001) J Physiol 530:21–33
43. Hodgkin AL, Keynes RD (1955) J Physiol 128:61–88
44. Zhou Y, MacKinnon R (2003) J Mol Biol 333:965–975
45. Zhou M, MacKinnon R (2004) J Mol Biol 338:839–846
46. Roux B, Allen T, Bernèche S, Im W (2004) Q Rev Biophys 37:15–103
47. Guidoni L, Carloni P (2002) Biochim Biophys Acta 1563:1–6
48. Blizniuk AA, Rendell AP (2004) J Phys Chem B 108:13866–13873
49. Compoint M, Ramseyer C, Huetz P (2004) Chem Phys Lett 397:510–515
50. Huetz P, Boiteux C, Compoint M, Ramseyer C, Girardet C (2006) J Chem Phys 124:44703–44712
51. Bucher D, Raugei S, Guidoni L, Dal Peraro M, Rothlisberger U, Carloni P, Klein ML (2006) Biophys Chem 124:292–301
52. Roux B, Bernèche S, Im W (2000) Biochemistry 39:13295–13306
53. Case DA, Darden TA, Cheatham TE III, Simmerling CL, Wang J, Duke RE, Luo R, Merz KM, Wang B, Pearlman DA, Crowley M, Brozell S, Tsui V, Gohlke H, Mongan J, Hornak V, Cui G, Broza P, Schafmeister C, Caldwell JW, Ross WS, Kollman PA (2004) AMBER 8. University of California, San Francisco
54. Brooks BR, Bruccoleri RE, Olafson BD, States DJ, Swaminathan S, Karplus M (1983) J Comp Chem 4:187–217
55. Bekker H, Berendsen HJC, Dijkstra FJ, Achterop S, van Drunen R, van der Spoel D, Sijbers A, Keegstra H, Reitsma B, Renardus MKR (1993) Gromacs: A parallel computer for molecular dynamics simulations In: de Groot RA, Nadrchal J (eds) Physics computing 92, World Scientific, Singapore
56. Phillips JC, Braun R, Wang W, Gumbart J, Tajkhorshid E, Villa E, Chipot C, Skeel RD, Kale L, Schulten K (2005) J Comp Chem 26:1781–1802
57. Holyoake J, Domene C, Bright JN, Sansom MSP (2004) Eur Biophys J 33:238–246
58. Frisch MJ, Trucks GW, Schlegel HB, Scuseria GE, Robb MA, Cheeseman JR, Montgomery Jr JA, Vreven T, Kudin KN, Burant JC, Millam JM, Iyengar SS, Tomasi J, Barone V, Mennucci B, Cossi M, Scalmani G, Rega N, Petersson GA, Nakatsuji H, Hada M, Ehara M, Toyota K, Fukuda R, Hasegawa J, Ishida M, Nakajima T, Honda Y, Kitao O, Nakai H, Klene M, Li X, Knox JE, Hratchian HP, Cross JB, Bakken V, Adamo C, Jaramillo J, Gomperts R, Stratmann RE, Yazyev O, Austin AJ, Cammi R, Pomelli C, Ochterski JW, Ayala PY, Morokuma K, Voth GA, Salvador P, Dannenberg JJ, Zakrzewski VG, Dapprich S, Daniels AD, Strain MC, Farkas O, Malick DK, Rabuck AD, Raghavachari K, Foresman JB, Ortiz JV, Cui Q, Baboul AG, Clifford S, Cioslowski J, Stefanov BB, Liu G, Liashenko A, Piskorz P, Komaromi I, Martin RL, Fox DJ, Keith T, Al-Laham MA, Peng CY, Nanayakkara A, Challacombe M, Gill PM W, Johnson B, Chen W, Wong MW, Gonzalez C, Pople JA (2004) Gaussian 03, Revision C02, Gaussian, Wallingford CT
59. Åqvist J, Luzhkov V (2000) Nature 404:881–884
60. Morais-Cabral JH, Zhou Y, MacKinnon R (2001) Nature 414:37–40
61. Bernèche S, Roux B (2003) Proc Natl Acad Sci USA 100:8644–8648
62. Perozo E, Cortes DM, Cuello LG (1999) Science 285:73–78
63. Allen TW, Chung SH (2001) Biochim Biophys Acta 1515:83–91
64. Chung SH, Allen TW, Kuyucak S (2002) Biophys J 82:628–645
65. Biggin PC, Sansom MSP (2002) Biophys J 83:1867–1876
66. Shrivastava IH, Sansom MSP (2002) Eur Biophys J 31:207–216
67. Shen Y, Kong Y, Ma J (2002) Proc Natl Acad Sci USA 99:1949–1953
68. Grottesi A, Domene C, Haider S, Sansom MSP (2005) IEEE Trans Nanobio 4:112–120
69. Compoint M, Picaud F, Ramseyer C, Girardet, C (2005) J Chem Phys 122:134707–134715
70. Liu YS, Sompornpisut P, Perozo E (2001) Nat Struct Biol 8:883–887
71. Compoint M, Picaud F, Ramseyer C, Girardet C (2005) Chem Phys Lett 407:199–204
72. Guidoni L, Torre V, Carloni P (2000) FEBS Lett 477:37–42
73. Compoint M, Boiteux C, Huetz P, Ramseyer C, Girardet C (2005) Phys Chem Chem Phys 7:4138–4145
74. Green ME (2002) J Biomol Struct Dyn 19:725–730
75. Sapronova A, Bystrov V, Green ME (2003) Theochem 630:297–307
76. Bernèche S, Roux B (2002) Biophys J 82:772–780
77. VanDongen AMJ (2004) Proc Natl Acad Sci USA 101:3248–3252
78. Bernèche S, Roux B (2000) Biophys J 78:2900–2917
79. Nelson PH (2002) J Chem Phys 117:11396–11403
80. Mafé S, Pellicer J, Cervera J (2005) J Chem Phys 122:204712–204720
81. Yesylevskyy SO, Kharkyanen VN (2004) Phys Chem Chem Phys 6:3111–3122
82. Kraszewski S, Boiteux C, Langner M, Ramseyer C (2006) Phys Chem Chem Phys 9:1219–1225
83. Boiteux C, Compoint M, Huetz P, Ramseyer C, Girardet C (2005) IEJMD 4:1–14
84. Compoint M, Carloni P, Ramseyer C, Girardet C (2004) Biochim Biophys Acta 1661:26–39
85. Consiglio JF, Andalib P, Korn SJ (2003) J Gen Physiol 121:111–124
86. Beckstein O, Sansom MSP (2003) Proc Natl Acad Sci USA 100:7063–7068
87. Saparov SM, Pohl P (2004) Proc Natl Acad Sci USA 101:4805–4809

88. Roux B, MacKinnon R (1999) Science 285:100–102
89. Senapati S, Chandra A (2001) J Phys Chem B 105:5106–5109
90. Molina ML, Encinar JA, Barrera FN, Fernandez-Ballester G, Riquelme G, Gonzalez-Ros JM (2004) Biochemistry 43:14924–14931
91. Encinar JA, Molina ML, Poveda JA, Barrera FN, Renart ML, Fernandez AM, Gonzalez-Ros JM (2004) FEBS Lett 579:5199–5204
92. Corry B, Vora T, Chung SH (2005) Biochim Biophys Acta 1711:72–86
93. Corry B, Chung SH (2006) Cell Mol Life Sci 63:301–315
94. Luzhkov VB, Åqvist J (2001) Biochim Biophys Acta 1548:194–202
95. Nimigean CM, Miller C (2002) J Gen Physiol 120:323–335
96. Bichet D, Grabe M, Jan YN, Jan LY (2006) Proc Natl Acad Sci USA 103:14355–14360
97. Noskov SY, Bernèche S, Roux B (2004) Nature 431:830–834
98. Shi N, Ye S, Alam A, Chen L, Jiang Y (2006) Nature 440:570–574
99. Asthagiri D, Pratt R, Paulaitis ME (2006) J Chem Phys 125:24701–24707
100. Ban F, Kusalik P, Weaver DF (2004) J Am Chem Soc 126:4711–4716
101. Singh UC, Kollman PA (1984) J Comp Chem 5:129–145
102. Besler BH, Merz KM, Kollman PA (1990) J Comp Chem 11:431–439
103. Hinsen K, Roux B (1997) J Comp Chem 18:368–380
104. Zhou Y, MacKinnon R (2004) Biochemistry 43:4978–4982
105. LeMasurier M, Heginbotham L, Miller C (2001) J Gen Physiol 118:303–313
106. Treptow W, Tarek M (2006) Biophys J 91:L26–L28